

A NEURAL MODEL OF THE LOCUST VISUAL SYSTEM FOR DETECTION OF OBJECT APPROACHES WITH REAL-WORLD SCENES

Matthias S. Keil*, Elisenda Roca-Moreno, Ángel Rodríguez-Vázquez

First published in:

Proceedings of the Fourth IASTED International Conference
Visualization, Imaging, and Image Processing
September 6-8, 2004, Marbella, Spain

ABSTRACT

In the central nervous systems of animals like pigeons and locusts, neurons were identified which signal objects approaching the animal on a direct collision course. Unraveling the neural circuitry for collision avoidance, and identifying the underlying computational principles, is promising for building vision-based neuromorphic architectures, which in the near future could find applications in cars or planes. At the present there is no published model available for robust detection of approaching objects under real-world conditions. Here we present a computational architecture for signalling impending collisions, based on known anatomical data of the locust *lobula giant movement detector* (LGMD) neuron. Our model shows robust performance even in adverse situations, such as with approaching low-contrast objects, or with highly textured and moving backgrounds. We furthermore discuss which components need to be added to our model to convert it into a full-fledged real-world-environment collision detector.

KEY WORDS

Locust, LGMD, collision detection, lateral inhibition, diffusion, ON-OFF-pathways, neuronal dynamics, computer vision, image processing

1 Introduction

It is essential to many animal species to recognize and avoid approaching predators. Animals like locusts or pigeons trigger collision avoidance behavior by relying exclusively on monocular information. Approaching objects give rise to an expanding image on the animal's retina, subtending a visual angle $\Theta(t)$. From $\Theta(t)$, both the expansion rate $\dot{\Theta}(t)$ and the angular acceleration $\ddot{\Theta}(t)$ can readily be computed. Object approaches with constant speed result in an approximately exponential increase in $\Theta(t)$ and $\dot{\Theta}(t)$. Such information may in principle be evaluated in the visual systems of pigeons and locusts, in order to trigger avoidance reactions. Whereas there is evidence that in pigeons three collision-sensitive variables are computed in parallel [1], the locust seems to compute only one [2, 3, 4].

Specifically, it has been found that responses of the *lobula giant movement detector* (LGMD) neuron correlate with object approaches [5, 6]. However, the type of "algorithm" implemented by the LGMD is a matter of ongoing debate, and currently prevailing hypothesis are suggesting contrasting points of view concerning the functional roles of *feedforward inhibition* (FFI) and *lateral inhibition* (LI), respectively [7, 8, 9] (notice that both types of inhibition act to suppress LGMD responses). With the first hypothesis it was suggested that FFI accounts for the LGMD's selectivity for approaching over receding objects, and for suppressing LGMD responses due to self-motion of the organism. A corresponding mechanism relies on the concurrent activation of a large number of local movement detectors (MDs) [10]. On the other hand, LI – in conjunction with excitation due to MDs – was proposed to implement a *critical race* over the LGMD "input cables" (dendrites) [11]: in the early phase of an object approach, and for translating objects, the activation of MDs over the photoreceptor arrays occurs linearly (or slower than linear) with time. Such activation patterns are canceled by laterally propagating inhibitory waves (these waves are triggered from previously activated MDs). The latter situation is different from the late phase of an object approach, where MDs are activated in a nearly exponential fashion. While the LI wave propagates with constant speed, the wavefront of MD activation spreads with continuous acceleration and thus can escape inhibition. Since the (uncanceled) MD activation directly excites the LGMD, it finally responds.

The second hypothesis was derived from the observation that LGMD responses to approaching objects could be fitted against an η -function, where $\eta(t) \propto \Theta \exp(-\alpha\Theta)$, and $\alpha = \text{const.}$ [12]. The η -function reveals an activity peak for objects approaching at constant velocity. Consequently, if the LGMD computed something like an η -function, then it would need to implement the multiplication operator. Indeed there is now neurophysiological evidence that multiplication of the excitatory input Θ with the (feedforward) inhibitory input $\exp(-\alpha\Theta)$ is performed by first logarithmically encoding both of the latter terms, before they are added in the LGMD neuron [13]. It seems that the logarithmic encoding is subsequently undone in the "output cable" (axon) of the LGMD by voltage-dependent sodium

*Corresponding author. Present address: Unversity of Barcelona, Faculty of Psychology, Barcelona, Spain. E-mail: matskeil[AT]ub.edu

conductances.

2 Model outline

Our approach is based on the aforementioned "critical race", and represents an improvement of a model previously presented in [14]. It processes information along two parallel streams, where one is sensitive for luminance increments occurring from time $t - 1$ to t (ON), and the other one is sensitive for luminance decrements (OFF). The ideal output of the model correlates with $\Theta(t)$ for object approaches (the nearer, the higher), and is zero for all remaining movement patterns (such as generated by translating objects, background movement, etc.). The model is sketched in figure 1.

2.1 ON- and OFF movement detectors

The input into the model is provided by video sequences. A frame of a sequence at time t corresponds to a luminance distribution $0 \leq \mathcal{L}(t) \leq 1$. A movement detector neuron p_{ij} at position (i, j) is defined by

$$\frac{dp_{ij}(t)}{dt} = -g_{leak}p_{ij} + \mathcal{L}_{ij}(t)(1 - p_{ij}) - \mathcal{L}_{ij}(t-1)(1 + p_{ij}) \quad (1)$$

where $g_{leak} = 100$ is a passive decay, which is related to the degree of low-pass filtering in time. It also implements saturation of p_{ij} with increasing input luminance. The output (or activity) of an ON-movement detector corresponds to positive values of p_{ij} , that is $\tilde{p}^{\oplus} \equiv [p]^+$, where $[\cdot]^+ \equiv \max(0, \cdot)$ denotes half-wave rectification. Negative values of p_{ij} encode OFF-activity, that is $\tilde{p}^{\ominus} \equiv [-p]^+$. Notice that, by convention, activities are always positive-valued. Conversely, we refer to (membrane-) *potential* to characterize a neuron's state. We observe that the potential or state of a neuron can be positive-valued and negative-valued.

2.2 Lateral inhibition

The "critical race" described above occurs between excitatory activities originating from movement detectors (equation 1), and laterally propagating inhibitory waves [11]. Laterally propagating waves are generated by nearest neighbor coupling such that adjacent neurons can exchange their membrane potential. In organisms, such coupling is established by electrical synapses or gap junctions. Mathematically, it is modeled by reaction-diffusion systems, which we call diffusion layers. There exists one diffusion layer ($s \in \{s^{\oplus}, s^{\ominus}\}$) for each pathway (ON and OFF):

$$\frac{ds_{ij}(t)}{dt} = g_{leak}(V_{rest} - s_{ij}) + g_{exc,ij}(1 - s_{ij}) + D \nabla^2 s_{ij} \quad (2)$$

where $g_{leak} = 10$ is related to the diffusion length constant of the system (e.g. [15]). $V_{rest} = -0.001$ is a resting potential (the value which is approached by s_{ij} without input). $D = 170$ is the diffusion coefficient, which specifies the speed of the propagation process. Finally, ∇^2 implements the Laplacian operator (we used a discrete four point approximation). ON- and OFF diffusion layer neurons receive excitatory input $g_{exc}^{\oplus} \equiv 250 \cdot [v^{\oplus}]^+$ and $g_{exc}^{\ominus} \equiv 250 \cdot [v^{\ominus}]^+$, respectively (excitatory units v are defined below). Diffusion layer outputs are given by $\tilde{s}^{\oplus} \equiv [s^{\oplus}]^+$ (ON) and $\tilde{s}^{\ominus} \equiv [s^{\ominus}]^+$ (OFF), respectively.

2.3 Summing units

Summing units are required to evaluate the result of the "critical race" between laterally propagating inhibition (provided by input $g_{inh,ij}$) and excitatory activity from movement detectors (provided by input $g_{exc,ij}$). Each pathway (i.e. ON and OFF) has its own layer of excitatory neurons:

$$\frac{dv_{ij}(t)}{dt} = g_{leak}(V_{rest} - v_{ij}) + g_{exc,ij}(1 - v_{ij}) - g_{inh,ij}(0.25 + v_{ij}) \quad (3)$$

where $g_{leak} = 100$, and $V_{rest} = -0.001$. Excitatory input into summing units is provided by ON- and OFF-movement detectors, respectively:

$$g_{exc,ij} = 250 \tilde{p} \cdot \exp(-\xi \tilde{s}_{ij}) \quad (4)$$

with a gain constant $\xi = 500$ (gain constants correspond to synaptic weights). Equation 4 establishes that diffusion layer activity \tilde{s}_{ij} decreases the excitatory input. In addition, diffusion layer activity drives the potential of the summing units away from the response threshold according to

$$g_{inh,ij} = \xi \tilde{s}_{ij} \quad (5)$$

The output of excitatory ON-units is given by $\tilde{v}^{\oplus} \equiv [v^{\oplus}]^+$, and $\tilde{v}^{\ominus} \equiv [v^{\ominus}]^+$ (OFF-unit). Notice that, in contrast to previous modeling attempts [11, 14], in the present approach feedback inhibition is used. In combination with equation 4, feedback inhibition ensures that the diffusion layers are not "drowned in activity" as a consequence of their small leakage conductances (c.f. equation 2; notice that the leakage conductance also specifies diffusion length, and therefore cannot be chosen arbitrarily high). The "drowning effect" typically occurs with feedforward circuits, where MD activity directly excites the diffusion layer. In the latter case, the presence of strong background movement in video sequences makes the model blind for subsequent object approaches.

2.4 LGMD neurons

Again, each pathway is associated with one LGMD. The ON-LGMD integrates activity from excitatory ON-units

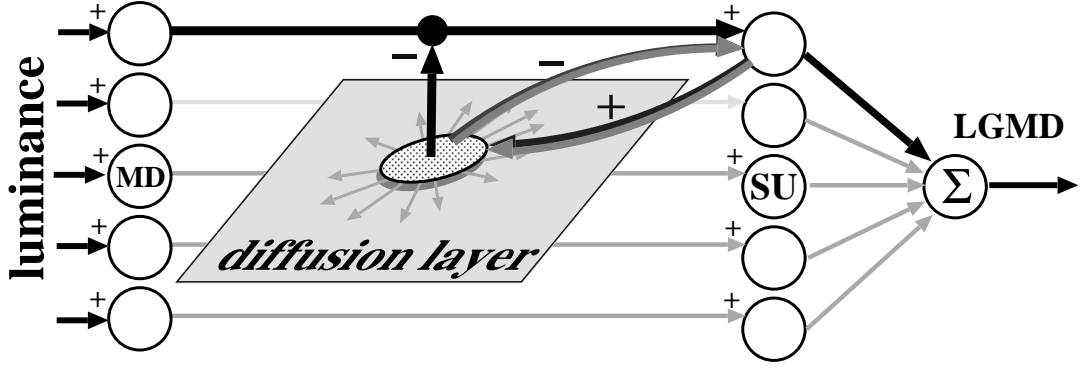


Figure 1. **Model diagram.** Movement information is extracted by movement detectors (MD, equation 1) from a series of *luminance* frames. MD output feeds into summing units (SUs, equation 3). SU output excites the *diffusion layer* (equation 2). Diffusion layer activity both decreases the input from MD into SU (vertical arrow, equation 4), and inhibits SUs (equation 5). Finally, the *LGMD* sums the activity of SUs. *LGMD* activity represents the model's output. Notice that there exist two independent pathways (ON and OFF) as the one sketched in the figure. Plus signs at arrows indicate excitation, and minus signs indicate inhibition. The horizontal arrow connecting the second (from above) MD with its corresponding SU has a lighter gray value only for reasons of improving the visualization.

$\tilde{v} \equiv \tilde{v}^{\oplus}$, and the OFF-LGMD neuron integrates activity from OFF-units $\tilde{v} \equiv \tilde{v}^{\ominus}$, according to

$$\mathcal{E} = \sum_{i,j}^n \tilde{v}_{ij} \quad (6)$$

The ON- and OFF-LGMD dynamics obeys (notice that l is a scalar variable)

$$\frac{dl(t)}{dt} = g_{leak}(V_{rest} - l) + \gamma_{ex}\mathcal{E}(t)(1 - l) \quad (7)$$

where $g_{leak} = 50$, and $V_{rest} = -0.001$. The output of the ON-LGMD is $\tilde{l}^{\oplus}(t) \equiv [l^{\oplus}(t)]^+$, and the output of the OFF-LGMD is $\tilde{l}^{\ominus}(t) \equiv [l^{\ominus}(t)]^+$. $\gamma_{ex} = 5 \cdot 128^2/n^2$ is a gain factor, which depends on the size of the luminance images (we used input images with n rows and n columns, see below).

3 Material and methods

All video sequences were coded with 8 bit resolution per pixel, and had equal numbers of rows and columns. Some of our video sequences had an unknown frame rate (*mcar* and *starwars*). The remaining videos (*softcrash*, *pedestrian*, and *highway*) were recorded with 25 frames per second. With each video sequence, we recorded activities of the ON-LGMD $\tilde{l}^{\oplus}(t)$ and OFF-LGMD $\tilde{l}^{\ominus}(t)$. In what follows, we give a brief description of each video (see also figure 2):

mcar The *mcar* video (resolution 285×285 pixels) shows an approaching car to a still observer. Since the observer does not move, no background movement is generated in this sequence.

starwars The *starwars* video (resolution 285×285 pixels) shows three approaching space ships. The background

is highly textured and moves in opposite direction to the space ships. The approaching space ships contrast only weakly with the background. This video also shows interlacing artifacts, and high frequency noise.

softcrash The *softcrash* video (resolution 150×150 pixels) was recorded from a driving car hitting a non-rigid obstacle.

pedestrian The *pedestrian* video (resolution 150×150 pixels) was recorded from a slowly driving car, where a pedestrian suddenly appears and runs across the scene.

highway The *highway* video (resolution 150×150 pixels) video was recorded from a car driving across a city highway. This video contains track changes, and other cars driving on adjacent lanes or ahead, respectively.

4 Results

Figures 3 to 7 show the output of the model for the various video sequences shown in figure 2. The *mcar* video represents the easiest test for the model, since there is virtually no background movement involved. Activities of both LGMDs (figure 3) smoothly follow the approaching car, where the curve for the ON-LGMD reaches a maximum before the OFF-LGMD. Triggering a collision alert in this case is rather easy, since one only needs to detect the rising phase of LGMD responses. Notice that both curves strongly resemble the η -function (see introduction).

Triggering a collision alert seems more difficult when monitoring LGMD activities with the *starwars* video (figure 4). At the beginning, a strong OFF-response, and a weaker ON-response are seen. These are transient effects, created by strong background movement. Since inhibitory

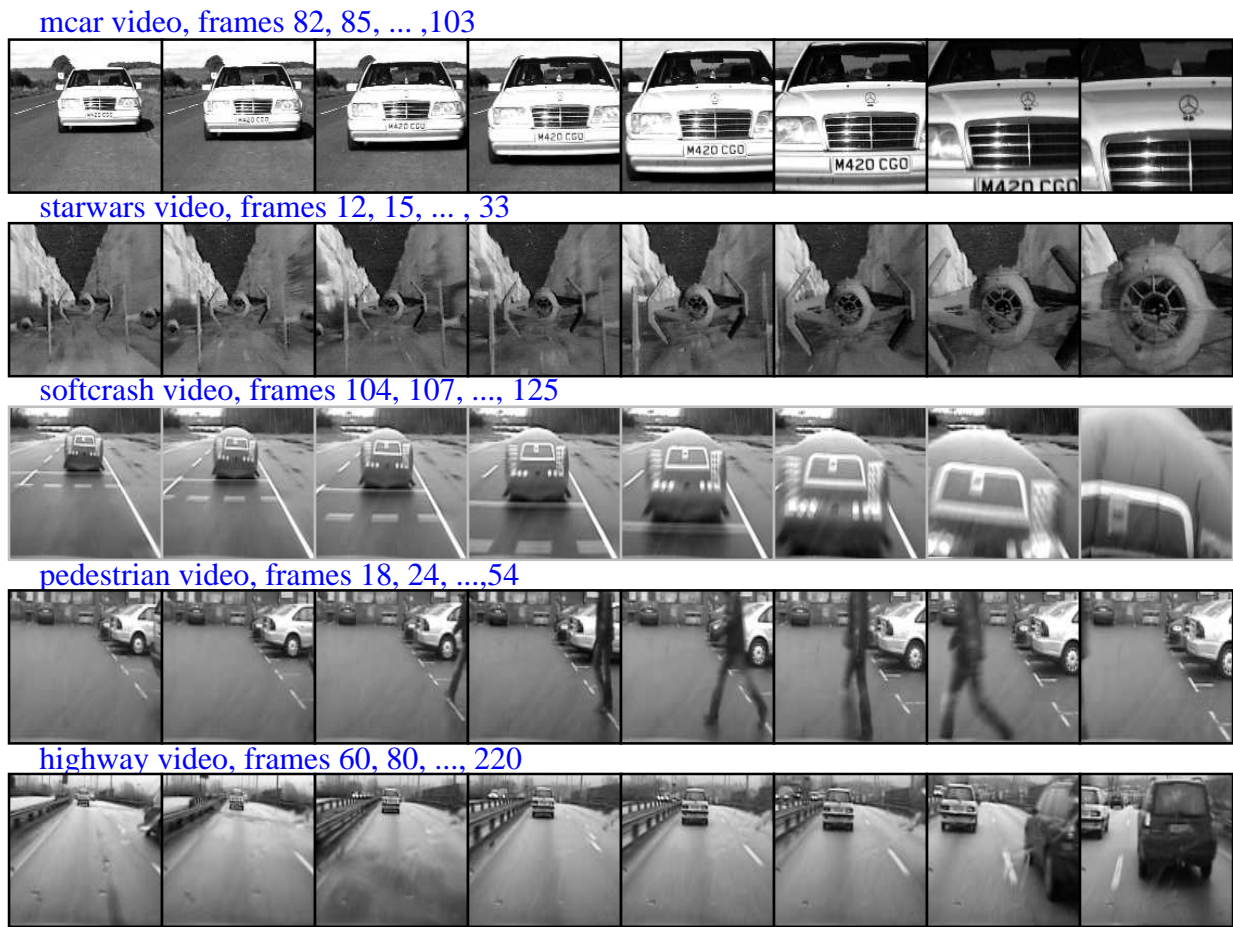


Figure 2. **Video sequences.** The figure shows single frames from the video sequences which were used for the simulations.

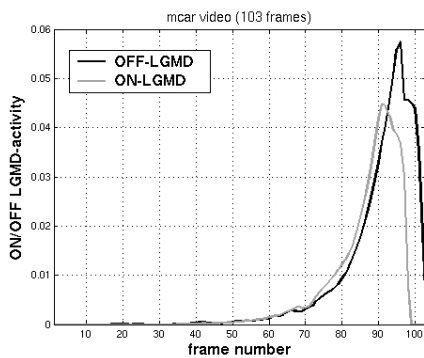


Figure 3. Results for the *mcar* video.

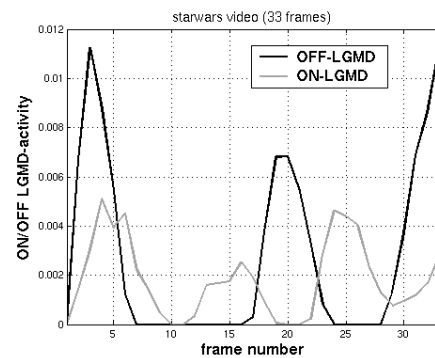


Figure 4. Results for the *starwars* video.

activity has not built up and spreaded laterally yet, background movement is not suppressed. The OFF-peak in the middle results from the approaching left and right space ship accompanying the middle one, as they move out of the scene. In the last frames, the OFF-response increases more strongly compared to the ON-response as the center space ship grows larger than the frame. The last ON-peak denotes the period where the lateral space ships have just moved out

of the scene (beginning) until the center space ship fills the whole frame (end). Hence, with the *starwars* video, collision detection is complicated because of the presence of secondary peaks. Both ON- and OFF-response amplitudes are substantially diminished by feedback inhibition.

The *softcrash* video (figure 5) shows several secondary response peaks in LGMD activities. These peaks reflect novel background activity (rising phase), which is caught

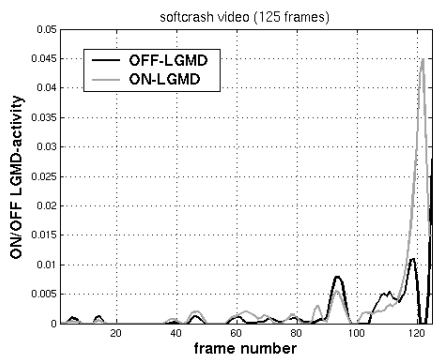


Figure 5. Results for the *softcrash* video.

up by lateral inhibition immediately (falling phase). The amplitudes of these peaks are relatively small and increase towards the collision event. The ON-LGMD response shows a pronounced maximum at collision time, what makes collision detection feasible in this situation.

The model may also serve to detect a pedestrian crossing

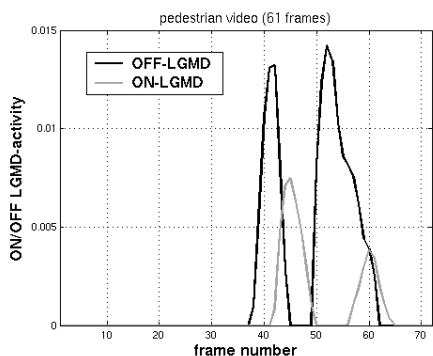


Figure 6. Results for the *pedestrian* video.

a scene (figure 6, *pedestrian* video). The model shows distinct response peaks when the pedestrian enters the scene. However, lateral inhibition soon suppresses corresponding responses. Since lateral inhibition cuts its own excitation by means of equation 4, response suppression occurs until inhibition dissipated, and subsequently LGMD responses may form again (second peak). Notice that since the car drives relatively slow, LGMD responses due to background movement can be neglected.

Ideally there would be no model response with the *highway* video (figure 7), because of the absence of any collision situation. All LGMD responses are due to background movement (such as street signs), cars passing by etc. This is reflected in the response amplitudes, which are comparatively small (c.f. figure 4), and are attenuated by lateral inhibition.

5 Discussion and conclusions

In this paper we presented an approach to collision detection, based on know neurophysiological data of the

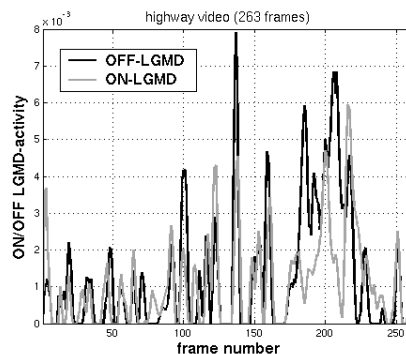


Figure 7. Results for the *highway* video.

lobula giant movement detector (LGMD). The present approach involves several improvements with respect to a previously presented model [14]. In the previous model, lateral inhibition was of feedforward type, that is movement detectors directly supported inhibition. The problem with the latter circuit is that strong background movement soon floods the diffusion layer associated with lateral inhibition. As a consequence, LGMD responses cease, and the model gets blind against object approaches. To remedy this problem, two parallel channels (ON and OFF) were introduced, with the goal to reduce the overall activity in diffusion layers. Furthermore, lateral inhibition within the present approach is of the feedback type, with the additional effect that once inhibition is active, it is cut off from its own excitation, such that it cannot grow further, but rather dissipates. In this way flooding of diffusion layers due to strong background movement is effectively reduced. Despite of it all, the present approach as it stands lacks several additional mechanisms.

First, the present model also responds to self-motion of agents. Such responses could possibly be attenuated by including feedforward inhibition, as described in the introduction. For automotive applications, it will be sufficient to include a detector for left and right movement (either visually by means of directional movement detectors, or by an external signal, e.g. from the steering wheel).

Second, a decision mechanism has to evaluate ON-LGMD and OFF-LGMD responses in order to detect a collision event or not. The results shown indicate that this is a non-trivial problem, since other situations than collisions may also trigger large LGMD responses (e.g. any sufficiently big object which approaches, but finally does not collide). Third, in order to make the model independent from object contrasts or illumination, adaptational mechanisms at the movement detector (or photoreceptor) level have to be included. Simple saturation of photoreceptor responses may only be a viable strategy if noise levels associated with luminance changes are negligible.

Acknowledgements

This work has been supported by the LOCUST project (IST2001-38097) and the VISTA project (TIC2003-09817-C02-01). The authors like to thank F.C.Rind for kindly providing the video sequences *mcar* and *starwars*, and Volvo Car Corporation for the video sequences *softcrash*, *pedestrian*, and *highway*.

References

- [1] H. Sun and B.J. Frost. Computation of different optical variables of looming objects in pigeon nucleus rotundus neurons. *Nature Neuroscience*, 1(4):296–303, 1998.
- [2] C.H.F Rowell. The orthopteran descending movement detector (DMD) neurones: a characterisation and review. *Zeitschrift für vergleichende Physiologie*, 73:167–194, 1977.
- [3] C.H.F Rowell. Variable responsiveness of a visual interneurone in the free-moving locust and its relation to behaviour and arousal. *Journal of Experimental Biology*, 55:748, 1977.
- [4] M. O’Shea and J.L.D. Williams. The anatomy and output connections of a locust visual interneurone: the lobula giant movement detector (lgmd) neurone. *Journal of Comparative Physiology*, 91:257–266, 1974.
- [5] F.C. Rind and P.J. Simmons. Orthopteran DCMD neuron: a reevaluation of responses to moving objects. I. Selective responses to approaching objects. *Journal of Neurophysiology*, 68(5):1654–1666, 1992.
- [6] F.C. Rind and P.J. Simmons. Orthopteran DCMD neuron: a reevaluation of responses to moving objects. II. Critical cues for detecting approaching objects. *Journal of Neurophysiology*, 68(5):1667–1682, 1992.
- [7] F.C. Rind and P.J. Simmons. Seeing what is coming: building collision-sensitive neurones. *Trends in Neuroscience*, 22(5):215–220, 1999.
- [8] F. Gabbiani, G. Laurent, N. Hatsopoulos, and H.G. Krapp. The many ways of building collision-sensitive neurons. *Trends in Neuroscience*, 22(5):437–438, 1999.
- [9] F.C. Rind and P.J. Simmons. Reply. *Trends in Neuroscience*, 22(5):438, 1999.
- [10] C.H.F. Rowell, M. O’Shea, and J.L.D. Williams. The neuronal basis of a sensory analyser, the acridid movement detector system.IV.The preference for small field stimuli. *Journal of Experimental Biology*, 68:157–185, 1977.
- [11] F.C. Rind and D.I. Bramwell. Neural network based on the input organization of an identified neuron signaling impending collision. *Journal of Neurophysiology*, 75:967–985, 1996.
- [12] N. Hatsopoulos, F. Gabbiani, and G. Laurent. Elementary computation of object approach by a wide-field visual neuron. *Science*, 270:1000–1003, 1995.
- [13] F. Gabbiani, H.G. Krapp, C. Koch, and G. Laurent. Multiplicative computation in a visual neuron sensitive to looming. *Nature*, 420:320–324, 2002.
- [14] M.S. Keil and A. Rodríguez-Vázquez. Towards a computational approach for collision avoidance with real-world scenes. In A. Rodríguez-Vázquez, D. Abbot, and R. Carmona, editors, *Proceedings of SPIE: Bioengineered and Bioinspired Systems*, volume 5119, pages 285–296, Maspalomas, Gran Canaria, Canary Islands, Spain, 19-21 May 2003. SPIE - The International Society for Optical Engineering.
- [15] J. Benda, R. Bock, P. Rujan, and J. Ammermüller. Asymmetrical dynamics of voltage spread in retinal horizontal cell networks. *Visual Neuroscience*, 18(5):835–848, 2001.